Switching Energy of Ferromagnetic Logic Bits

Behtash Behin-Aein, *Student Member, IEEE*, Sayeef Salahuddin, *Member, IEEE*, and Supriyo Datta, *Fellow, IEEE*

***Abstract*—Power dissipation in switching devices is believed to be the single most important roadblock to the continued downscaling of electronic circuits. There is a lot of experimental effort at this time to implement switching circuits based on magnets and it is important to establish power requirements for such circuits and their dependence on various parameters. This paper analyzes switching energy that is dissipated in the switching process of single-domain ferromagnets used as *cascadable logic* bits. We obtain generic results that can be used for comparison with alternative technologies or guide the design of magnet-based switching circuits. Two central results are established. One is that the switching energy drops significantly if the ramp time of an external pulse exceeds a critical time. This drop occurs more rapidly than what is normally expected of adiabatic switching for a capacitor. The other result is that under the switching scheme that allows for logic operations, the switching energy can be described by a single equation in both fast and slow limits. Furthermore, these generic results are used to discuss the practical consideration such as dissipation versus speed, increasing the switching speed and scaling. It is further explained that nanomagnets can have scaling laws similar to CMOS technology.**

***Index Terms*—Adiabatic pulse, cascadable logic, critical ramp time, fast pulse, Landau–Lifshitz–Gilbert equation (LLG), magnetic quantum cellular automata (MQCA), nanomagnet, switching energy.**

I. Introduction

IT HAS been suggested [1] that the use of collective systems like a magnet can reduce the intrinsic switching energy (that is dissipated throughout switching) significantly compared to that required for individual spins. There is also a lot of experimental effort [2]–[7] at this time to implement switching circuits based on magnets. There has been some work [8] on modeling magnetic circuits like magnetic quantum cellular automata (MQCA) in the atomic scale using quantum density matrix equation but most of the work [9]–[13] is in the classical regime using the well-known micromagnetic simulators (object-oriented micromagnetic framework, OOMMF) based on the Landau–Lifshitz–Gilbert (LLG) [15]–[17] equation. This paper too is based on the LLG equation, but our focus is not on obtaining the energy requirement of any specific device in a particular simulation. Rather it is to obtain generic results that can guide the design of magnet-based switching circuits as well as providing a basis for comparison with alternative technologies.

Manuscript received April 7, 2008; revised November 16, 2008. First published March 10, 2009; current version published July 9, 2009. This work was supported by the Nanoelectronics Research Initiative (NRI). The review of this paper was arranged by Associate Editor D. Litvinov.

B. Behin-Aein and S. Datta are with the School of Electrical and Computer Engineering and National Science Foundation (NSF) Network for Computational Nanotechnology (NCN), Purdue University, West Lafayette, IN 47907 USA.

S. Salahuddin is with the School of Electrical Engineering and Computer Science, University of California (UC) Berkeley, Berkeley, CA 94720 USA.

Color versions of one or more of the figures in this paper are available online at http://ieeexplore.ieee.org.

Digital Object Identifier 10.1109/TNANO.2009.2016657

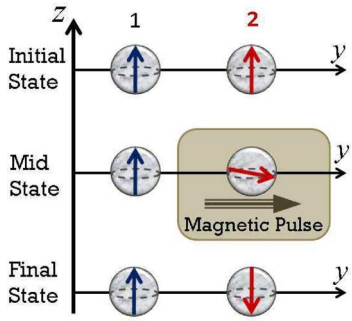

Fig. 1. Magnetic pulse is applied to magnet 2, provides energy, and places it along its hard axis (along y), where a small bias field due to magnet 1 can tilt it upward or downward thereby dictating its final state on removing the pulse.

The results we present are obtained by analyzing the cascadable switching scheme illustrated in Fig. 1, where the magnet to be switched (magnet 2) is first placed along its hard axis by a magnetic pulse (see "mid state" in Fig. 1). On removing the pulse, it falls back into one of its low-energy states (up or down) determined by the "bias" provided by magnet 1. What makes this scheme specifically suited for logic operations is that it puts magnet 2 into a state determined by magnet 1 (thereby transferring information), but the energy needed to switch magnet 2 comes largely from the external pulse and *not* from magnet 1. This is similar to conventional electronic circuits where the energy needed to charge a capacitor comes from the power supply, although the information comes from the previous capacitors. This feature seems to be an essential ingredient needed to *cascade logic units*. To our knowledge, the switching scheme shown in Fig. 1 was first discussed by Bennet [18] and is very similar to the schemes described in many recent publications (see, e.g., Likharev and Korotkov [19], Kummamuru *et al.* [20], and Csaba *et al.* [9]).

This paper uses the LLG equation to establish two central results. One is that the switching energy drops significantly as the ramp time τ_r of the magnetic pulse exceeds a critical time τ_c given by (14). This is similar to the drop in the switching energy of an *RC* circuit when $\tau_r \gg RC$. But the analogy is only approximate since the switching energy for magnets drops far more abruptly with increasing τ_r. The significance of τ_c is that it quantifies how slow a pulse needs to be in order to qualify as "adiabatic," and thereby, reduce dissipation significantly. Considering typical magnets used in the magnetic storage industry, and using ramp times of a few τ_c, intrinsic switching frequency of 100 MHz to 1 GHz can easily be in the adiabatic regime of switching where intrinsic dissipation of magnets is very small.

Interestingly, we find that the switching energy for the trapezoidal pulses investigated in this paper in both the "fast" and "slow" limits can be described by a single equation [(8)], which is the other central result of this paper. Later in this paper

(Section IV), we will discuss how (14) and (8) can be used to guide scaling and increase switching speeds. Furthermore, these equations can be used to compare magnet-based switching circuits with alternative technologies.

It has to be emphasized that dissipation of the external circuitry also has to be evaluated for any new technology. A careful evaluation would require a consideration of actual circuitry to be used (see, e.g., [13] and [14]) and is beyond the scope of this paper. However, following Nikonov *et al.*. [14], if a wire coil is used to produce the pulse, we can estimate the energy dissipated in creating the field $H_{\rm pulse}$ as $(H_{\rm pulse}^2/2)(V/Q)$ in CGS system of units. Q is the quality factor of the circuit and V is the volume over which the field extends. Depending on Q, V, and $H_{\rm pulse}$, the dissipated energy can be much larger, comparable to or much smaller than Ku_2V (see Section II), which is the energy barrier of a magnet and sets the energy scale for the effects considered here in this paper.

Overview of the paper: As mentioned earlier, our results are based on direct numerical simulation of the LLG equation. However, we find that in two limiting cases, it is possible to calculate switching energy simply using the energetics of magnetization, and these limiting results are described in Sections II and III, which are related to (8). In Section IV, we use the LLG equation to show that the switching energy drops sharply for ramp times larger than the critical time given by (14). In Section V, using coupled LLG equations, we analyze a chain of inverters to show that the total dissipation increases linearly with the number of nanomagnets thus making it reasonable to use the one-magnet results in our paper to evaluate complex circuits, at least approximately. Finally, in Section VI, practical issues such as dissipation versus speed, increasing the switching speed and scaling are qualitatively discussed in the light of these results.

II. Dissipation With Fast ($\tau_r \ll \tau_c$) Pulse

Before we get into the discussion of switching energy, let us briefly review the energetics of a magnet. The energy of a magnet with an effective second order uniaxial anisotropy can be described by $E/V = Ku_2 \sin^2(\theta)$, where θ measures the deflection from the easy axis that we take as the z-axis. All isotropic terms have been omitted because they do not affect dynamics and hence dissipation of the magnet.[1] There are two magnetic fields that control the switching (see Fig. 1). The external pulse $H_{\rm pulse}$ and the bias field $H_{\rm dc}$ due to the neighboring magnet. Including the internal energy and the interaction energy of magnetic moment with external fields, the energy equation reads

$$\frac{E}{V} = -M_s \hat{m} \cdot \vec{H}_{\rm pulse} + Ku_2 \sin^2(\theta) - M_s \hat{m} \cdot \vec{H}_{\rm dc}$$

where M_s is the saturation magnetization that is equivalent to the magnetic moment per unit volume if the unit volume is magnetized to saturation, $\hat{m}$ is a unit vector in the direction of magnetization, V is the volume of the magnet, and Ku_2 is the second-order anisotropy constant with dimensions of energy per unit volume. The applied field $H_{\rm pulse}$ is along the hard axis $\hat{y}$, the bias field $H_{\rm dc}$ is along the easy axis $\hat{z}$ so the energy equation becomes

$$\frac{E}{V} = -M_s H_{\rm pulse} \sin(\theta)\sin(\phi) + Ku_2 \sin^2(\theta) - M_s H_{\rm dc} \cos(\theta) \tag{1}$$

where ϕ is defined as in a standard spherical coordinate system. Using (1), we will show that dissipation with a fast pulse (small ramp time) can be written as

$$E_d = \left(\frac{H_{\rm pulse}}{H_c}\right)^2 (2Ku_2V), \qquad \text{for } H_{\rm pulse} \le H_c \tag{2a}$$

$$E_d = 2Ku_2V, \qquad \text{for } H_{\rm pulse} = H_c \tag{2b}$$

$$E_d = \left(\frac{H_{\rm pulse}}{H_c}\right) (2Ku_2V), \qquad \text{for } H_{\rm pulse} \ge H_c. \tag{2c}$$

For reasons to be explained, under the condition of (2a), the logic device will not work. Nevertheless, this equation is useful for determining dissipation in the adiabatic limit. In the earlier equations, $H_c \equiv 2Ku_2/M_s$ is the minimum field necessary to put the magnet along its hard axis. Notice that the bias field $H_{\rm dc}$ is a dc field coming from the neighboring magnet. In practice, whether the bias field is a dc field or not, its magnitude has to be larger than noise such that when the magnet is put along its hard axis as in Fig. 1, the bias field can deterministically tilt the magnet toward its direction. We will show in Section II-B that for $H_{\rm dc} \le 0.1H_c$, dissipation can still be calculated using (2).

To derive (2), we find the initial and final state energies under various conditions and evaluate the difference. We have to emphasize that all these states essentially pertain to the energy minima (equilibrium states), i.e., they are either the minimum of energy or they represent a nonequilibrium state instantaneously after the equilibrium state (minimum of energy) has changed. Since all the fields considered here are in the y–z plane and no out-of-plane field is considered, the equilibrium states (the energy minima) will always lie in the y–z plane for which $\phi = 90^\circ$.

A. Zero Bias Field ($H_{\rm dc} = 0$)

Fig. 2 is plotted using (1) with $\phi = 90^\circ$ and $H_{\rm dc} = 0$, which is the first case to be discussed. The different contours correspond to different values of $H_{\rm pulse}$.

Derivation of (2b): Let us start with (2b), which is the most important and also easiest to derive. Dissipation occurs both during turn-ON and turn-OFF of the pulse and the overall switching energy is sum of the two, in general. The dashed contour in Fig. 2 corresponds to $H_{\rm pulse} = H_c$, which is the minimum value needed to make $\theta = 90^\circ$ (point 2) the energy minimum. For a pulse with fast ($\tau_r \ll \tau_c$) *turn*-ON, dissipation can be calculated using (1) as the difference between the initial and the final state energies that are given by point 1 (or 4) and point 2 on the dashed contour. This value is

$$E_{1(4)} - E_2 = Ku_2V.$$

[1]The isotropic terms, like the demagnetizing field for a sphere or the Weiss field have not been taken into account because they can be expressed as $\lambda\vec{M}$, where $\vec{M}$ is the magnetization and λ is an scalar. Based on the LLG equation, fields of this form will *not* alter the dynamics of magnetization and have no bearing on dissipation.

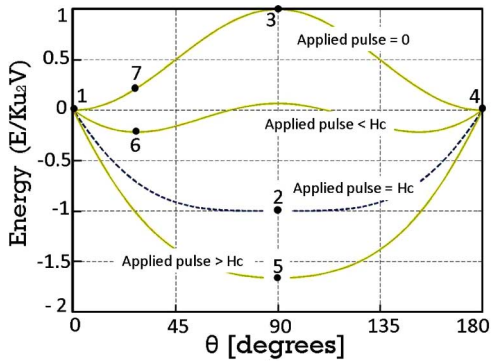

Fig. 2. Energy landscape of the magnetization under various applied fields. For fast turn-ON of the pulse to H_c, dissipation is equal to the barrier height (magnet relaxes from point 1 (or 4) to point 2). When the field is turned OFF fast, magnet relaxes from point 3 to point 4 (or 1) depending on any infinitesimal bias again dissipating an amount equal to the barrier height. Similar arguments explain the dissipation with pulses more and less than H_c.

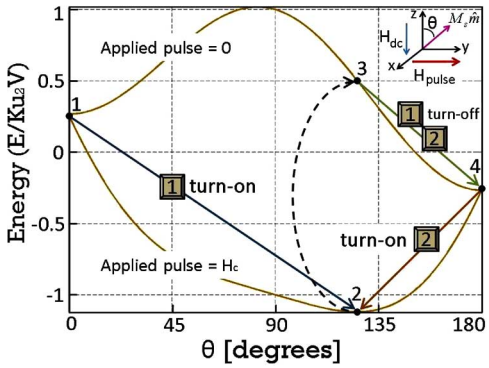

Fig. 3. Energy landscape of magnetization with bias field $H_{\rm dc}$ in the $-z$-direction for two values of the pulse: 0 and H_c. Upon *turn*-ON, if magnetization starts from $\theta = 0^\circ$ (*case 1*), it drops from point 1 ($E = +M_s V H_{\rm dc}$) to point 2 dissipating the difference. If it starts from $\theta = 180^\circ$ (*case 2*), it drops from point 4 ($E = -M_s V H_{\rm dc}$) to point 2 dissipating the difference. Upon *turn*-OFF, both cases 1 and 2 drop from point 3 to point 4 dissipating the difference.

For a pulse with fast ($\tau_r \ll \tau_c$) *turn*-OFF, the energy contour immediately changes from the dashed one to the uppermost one in Fig. 2. Under any infinitesimal bias, magnetization falls down the barrier to the left (relaxing to point 1) or to the right (relaxing to point 4) giving a dissipation of

$$E_3 - E_{1(4)} = Ku_2 V$$

equal to the turn-ON dissipation. The switching energy (*total dissipation*) is sum of the values for turn-ON and turn-OFF that gives us (2b).

Derivation of (2c): This is the case with $H_{\rm pulse} > H_c$. The bottom-most energy contour in Fig. 2 shows such a situation as an example. The minimum of energy is still at $\theta = 90^\circ$ (point 5), however, now the energy well is deeper. For a pulse with fast ($\tau_r \ll \tau_c$) *turn*-ON, dissipation is the difference between the initial and final state energies

$$E_{1(4)} - E_5 = (M_s H_{\rm pulse} - Ku_2)V$$

where E_5 is used as a generic notation for the bottom of any well with $H_{\rm pulse} > H_c$. For a pulse with fast ($\tau_r \ll \tau_c$) *turn*-OFF, the energy contour immediately changes from the bottom most curve to the uppermost curve in Fig. 2. Depending on any infinitesimal bias, magnet will relax from point 3 to either point 1 or 4 dissipating the difference

$$E_3 - E_{1(4)} = Ku_2 V.$$

The switching energy is sum of the values for turn-ON and turn-OFF, which with straightforward algebra gives us (2c).

Derivation of (2a): With $H_{\rm pulse} < H_c$, magnetization will not align along its hard axis ($\theta = 90^\circ$). This can be seen in Fig. 2, where for a pulse lower than H_c there are two minima of energy (see, e.g., point 6) not located along the hard axis. The logic device will not work in this regime because it needs to be close to its hard axis so that the field of another magnet can tilt it toward one minima deterministically. Nevertheless, we derive dissipation for these pulses because we use the results in Section III-A to show switching energy in the adiabatic limit. For a pulse with fast ($\tau_r \ll \tau_c$) *turn*-ON, dissipation is the difference between the initial and final state energies

$$E_1 - E_6 = \left(\frac{M_s H_{\rm pulse}}{2Ku_2}\right)^2 (Ku_2 V). \tag{3}$$

For a pulse with fast ($\tau_r \ll \tau_c$) *turn*-OFF, the energy contour suddenly becomes the uppermost one in Fig. 2. At that moment, magnetization is still at the same θ (point 7). It follows down the barrier (to point 1) with the dissipation given by

$$E_7 - E_1 = \left(\frac{M_s H_{\rm pulse}}{2Ku_2}\right)^2 (Ku_2 V). \tag{4}$$

The *total dissipation* is sum of the values for turn-ON and turn-OFF that results in (2a).

B. Nonzero Bias Field ($H_{\rm dc} \neq 0$)

In this section, we show that for $H_{\rm pulse} = H_c$, so long as $H_{\rm dc} \leq 0.1 H_c$ switching energy can be calculated fairly accurately using (2b) considering only the effect of $H_{\rm pulse}$. For $H_{\rm pulse} > H_c$, the effect of $H_{\rm dc}$ is even less pronounced as compared to $H_{\rm pulse}$ and (2c) can be used to calculate dissipation. Again, we are interested in initial and final state energies that can be calculated using (1) with $\phi = 90^\circ$. $H_{\rm dc}$ can be positive (along z) or negative (along $-z$). Fig. 3 shows the energy landscape with an $H_{\rm dc}$ in the $-z$-direction. If $H_{\rm dc} \neq 0$, then the up and down states (points 1 and 4) of the magnet have different initial energies that result in two different cases to be analyzed. *Case 1* designates the situation where initial magnetization (point 1) and $H_{\rm dc}$ are in the *opposite* direction. *Case 2* designates the situation where initial magnetization (point 4) and $H_{\rm dc}$ are in the *same* direction.

For a pulse with fast ($\tau_r \ll \tau_c$) *turn*-ON, *case 1* dissipates the difference between points 1 and 2 and *case 2* dissipates the difference between points 4 and 2. When the pulse is suddenly turned OFF, in both cases magnetization finds itself at point 3, drops down to point 4, and dissipates the difference. It is not possible to give an exact closed-form expression for the value of dissipation with nonzero bias. Instead, based on numerical calculations, we show figures that provide useful insight to

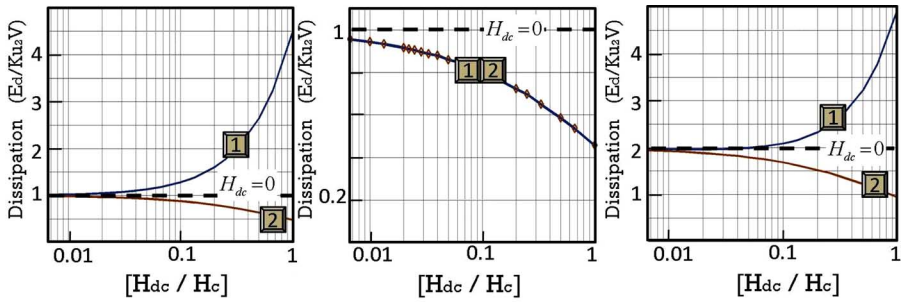

Fig. 4. (a) *Turn*-ON dissipation with nonzero bias. Cases 1 and 2 correspond to different initial directions of magnetization (see Fig. 3). The dashed line depicts the value of dissipation with zero bias. (b) *Turn*-OFF dissipation with nonzero bias. Both cases 1 and 2 dissipate the same amount (see Fig. 3). (c) Total dissipation with nonzero bias. Notice that for relevant (small) values of $H_{\rm dc}/H_c$, total dissipation of both cases 1 and 2 is close to the value $2Ku_2V$, which is the same as the case with infinitesimal bias.

conclude that for pulses with fast ramp time the effect of bias on switching energy is negligible.

The energy of point 2 (and subsequently, point 3) depicted in Fig. 3 changes as the relative magnitude of $H_{\rm dc}$ and H_c are changed. We like to know how dissipation changes as a function of the ratio $H_{\rm dc}/H_c$. The numerical results are plotted in Fig. 4 using (1). Fig. 4(a) shows that for a pulse with fast *turn*-ON and small values of $H_{\rm dc}/H_c$, both cases dissipate about Ku_2V. As this ratio is increased, the energy separation between points 1 and 2 (see Fig. 3) increases and that of points 4 and 2 decreases that results in higher dissipation of *case 1* and lower dissipation of *case 2*. Fig. 4(b) shows the dissipation for a pulse with fast *turn*-OFF, which is less than the barrier height Ku_2V, and is expected because under the presence of $H_{\rm dc}$, after turn-ON, magnetization ends up closer to the final state (see Fig. 3) as compared to the case where $H_{\rm dc}=0$ (see Fig. 2). The switching energy is sum of the dissipation values for turn-ON and turn-OFF plotted in Fig. 4(c). For $H_{\rm dc}=H_c$, the bias field $H_{\rm dc}$ alone can switch the magnet and it is completely an unwanted situation.[2] Note that for practical purposes, values of $H_{\rm dc}$ are small compared to H_c (for instance $H_{\rm dc}\leq 0.1H_c$) and the switching energy is more or less about $2Ku_2V$ that gives us (2b). For $H_{\rm pulse}>H_{\rm dc}$, the effect of bias is even less pronounced and switching energy can be calculated using (2c).

III. Dissipation With Adiabatic ($\tau_r \gg \tau_c$) Pulse

We have seen in Section II that for pulses with fast ramp times, the effect of bias ($H_{\rm dc}$) is negligible for $H_{\rm dc}\leq 0.1H_c$ and switching energy is obtained fairly accurately even if we set $H_{\rm dc}=0$. By contrast, for pulses with slow ramp time, switching energy can be made arbitrarily small for $H_{\rm dc}=0$ and the actual switching energy is determined entirely by the $H_{\rm dc}$ that is used. In this section, we will first show why the switching energy can be arbitrarily small for $H_{\rm dc}=0$ and then show that for $H_{\rm dc}\neq 0$ it will saturate in *case 1* (see Fig. 3) but can be made arbitrarily small in *case 2*[3] (see Fig. 3)

$$E_d=\left(\frac{2H_{\rm dc}}{H_c}\right)^p (2Ku_2V)\,(\text{case 1}) \tag{5}$$

$$E_d\to 0 \qquad (\text{case 2})\,. \tag{6}$$

Two points are in order. First, the analysis presented here is exact in the absence of noise. If thermal noise is present the analysis may not be true in general and needs to be modified accordingly. Second, if in the process of switching an information bit is destroyed, as in two inputs and one output gates (e.g., AND/OR), then there will be a finite switching energy even for adiabatic switching [25].

A. Zero Bias Field ($H_{\rm dc}=0$)

Gradual *turn*-ON of the pulse corresponds to increasing the pulse in many small steps. Fig. 5(a) shows the energy landscape. As the field is gradually turned ON, the energy contours change little by little from top to bottom. The minimum of energy gradually shifts from point 1 (or 4) to point 2. Magnetization hops from one minimum of energy to the other. But why is it that gradual turn-ON of the pulse dissipates less than sudden turn-ON?

If the external pulse is turned ON to H_c in N equal steps, we show that there is equal amount of dissipation at each step. Then total dissipation is N times that of each step. We show that dissipation of each step is proportional to $1/N^2$; hence, as the number of steps increases, dissipation decreases as $1/N$ and in the limit of $N\to\infty$, $E_d\to 0$ (this is not unlike a similar argument that has been given for charging up a capacitor adiabatically [26]). At each step when the pulse is increased by $\Delta H=H_c/N$, the dissipated energy is the difference between initial and final state energies. Such a situation is illustrated in Fig. 5(a) where "a" denotes a minimum on an energy contour corresponding to H_n (magnitude of the pulse after n steps).

[2]In principle, magnet A can switch magnet B unidirectionally with no need for an external pulse given that: $Ku_{2,A}V_A > (M_{sA}V_A)\,(M_{sB}V_B)/r^3 > Ku_{2,B}V_B$ holds. This entails designing circuits with magnets of different parameters (e.g., volume) so no two magnets in the circuit can have the same parameters; not to mention the complexities caused by the fields exerted from other neighbors.

[3]This essentially states that it is not a matter of principle that interacting magnets must have saturating dissipation as was previously suggested [11]. This is also shown by analyzing the dissipation of a chain of coupled magnets where for some configurations dissipation arbitrarily goes down whereas for some other configurations it saturates. The concepts behind such effects can easily be traced back to the two cases (1 and 2) discussed in the context of one magnet and a bias field $H_{\rm dc}$.

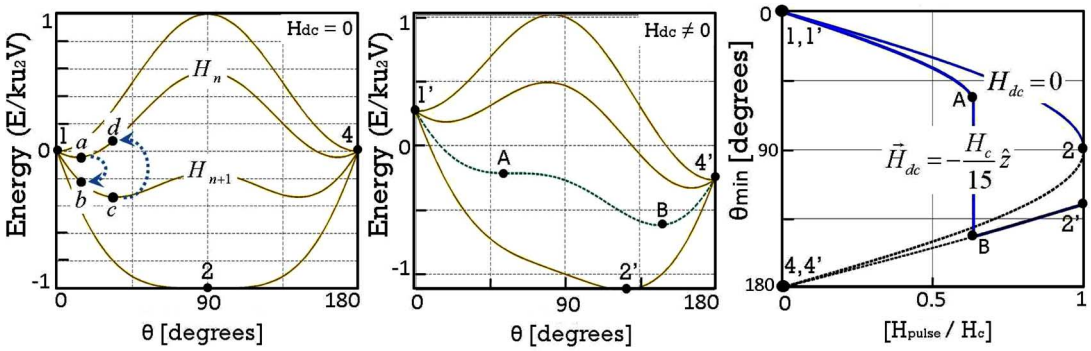

(a) (b) (c)

Fig. 5. (a) Energy landscape of magnetization as pulse is increased from 0 (top curve) to H_c (bottom curve) with $H_{\rm dc} = 0$. (b) Energy landscape of magnetization as pulse is increased from 0 (top curve) to H_c (bottom curve) with $H_{\rm dc} \neq 0$ in the $-z$-direction. (c) Adiabatic progression of ground state in the presence of a bias field $H_{\rm dc}$ in the $-z$-direction. Figure shows those values of θ that minimize energy as the pulse is adiabatically ramped from 0 to 1 and back to 0. Consider the $H_{\rm dc} \neq 0$ case. If the magnetization starts at point $1'$, it moves to point A along the solid line, then suddenly drops down to point *B*; as $H_{\rm pulse}$ is further increased, it moves to point $2'$ where $H_{\rm pulse} = H_c$. As $H_{\rm pulse}$ is decreased back to 0, magnetization moves along the solid line from $2'$ to B and then along the dashed line to point $4'$. Fig. 5(b) and (c) can be used in conjunction to assist understanding.

When the pulse is stepped up to H_{n+1}, magnetization suddenly finds itself at point "b" (initial state) and falls down to "c" (final state). Note that dissipation is $E_b - E_c$ and not $E_a - E_c$. This is because when the field suddenly changes from H_n to H_{n+1}, magnet has not had time to relax and dissipate energy. Here, we use E_b and E_c as generic notations for initial and final energy of any step. E_b can be found by finding the θ that corresponds to point "a" (the minimum of energy with $H_{\rm pulse} = H_n$) and substituting it in (1) with $H_{\rm pulse} = H_{n+1}$. After some straightforward algebra, we get $E_b = -(M_s V)H_{n+1}\,(M_s H_n/2Ku_2) + (Ku_2 V)\,(M_s H_n/2Ku_2)^2$. Equation (3) can be used to calculate $E_c = -\,(M_s H_{n+1}/2Ku_2)^2\,(Ku_2 V)$. Using the identities $H_{n+1} = H_n + \Delta H$ and $\Delta H = H_c/N$, the dissipated energy per step is obtained as

$$E_d^{\rm step} = E_b - E_c = Ku_2 V\left(\frac{1}{N^2}\right).$$

For gradual *turn*-OFF consider points c, d, and a. When $H_{\rm pulse} = H_{n+1}$, magnetization is at c and after the pulse is decreased by one step to H_n, it finds itself at "d", falls down to "a" dissipating the difference $E_d - E_a$. E_d can be found by finding the θ that corresponds to point "c" (the minimum of energy with $H_{\rm pulse} = H_{n+1}$) and substituting it in (1) with $H_{\rm pulse} = H_n$, we get $E_d = -(M_s V)H_n\,(M_s H_{n+1}/2Ku_2) + (Ku_2 V)\,(M_s H_{n+1}/2Ku_2)^2$. Again, (3) can be used to give $E_a = -\,(M_s H_n/2Ku_2)^2\,(Ku_2 V)$. Using the identities $H_{n+1} = H_n + \Delta H$ and $\Delta H = H_c/N$, we obtain for the dissipated energy per step

$$E_d^{\rm step} = E_d - E_a = Ku_2 V\left(\frac{1}{N^2}\right).$$

The switching energy is sum of the dissipation values for *turn*-ON, $E_d = Ku_2 V/N$, and *turn*-OFF, $E_d = Ku_2 V/N$, which in the limit of $N \to \infty$, tends to 0 ($E_d \to 0$).

B. Nonzero Bias Field ($H_{\rm dc} \neq 0$)

For *turn*-ON let us consider *case 1* first where initial magnetization and $H_{\rm dc}$ are in opposite directions [point $1'$ in Fig. 5(b)]. As the field is gradually turned ON, magnetization starts from point $1'$ and hops from one minimum of energy to the next. Increasing the number of steps brings the minima closer to each other so that magnetization stays in its ground state while being switched. However, when magnetization gets to point A, situation changes. At that point the energy barrier that formerly separated the two minima on the two sides disappears. Magnetization falls down from point A to B and dissipates the energy difference. This sudden change in the minimum of energy occurs no matter how slow the pulse is turned ON and causes the switching energy to saturate so long as $H_{\rm dc} \neq 0$. Quantitatively, this can be seen by plotting $\theta_{\rm min}$ versus $H_{\rm pulse}$ [Fig. 5(c)] using equation (1). When the left solid curve is traced from $\theta_{\rm min} = 0$, it is evident that there is a discontinuous jump in the $\theta_{\rm min}$ values that minimize energy. This discontinuity goes away only when $H_{\rm dc} = 0$ (right solid curve). In *case 2*, magnetization starts from point $4'$, i.e., $\theta_{\rm min} = 180^\circ$ [see Fig. 5(b) and (c)], gets to point B at which there is *no* sudden change of minimum and as the pulse is increased further to H_c, it gradually moves to point $2'$. During *turn*-OFF in both cases 1 and 2, magnetization gradually moves from [see Fig. 5(c)] point $2'$ to B and then finally to point $4'$ all along staying in its minimum of energy with no discontinuity. Dissipation tends to zero as the pulse is turned OFF in infinitesimal steps.

In the slow limit, the entire dissipation is determined by the energy difference between points A and B, $E_A - E_B$ in Fig. 5(b). For a given $H_{\rm dc}$, one has to find that particular value of $H_{\rm pulse}$ for which the local energy maximum in the middle disappears which means that the second derivative of energy with respect to θ must be zero (no curvature). Since magnetization has been in the minimum of energy while getting to point A, first derivative of energy with respect to θ must also be equal to zero. Under these conditions, the value of θ at A, and subsequently, E_A can be found using (1). E_B can be found as the actual minimum of energy from (1) where the first derivative of energy with respect to θ is zero but the second derivative is not. What affects $E_A - E_B$ is the relative magnitude of $H_{\rm dc}$ and H_c. It is not possible to give an analytical closed-form expression

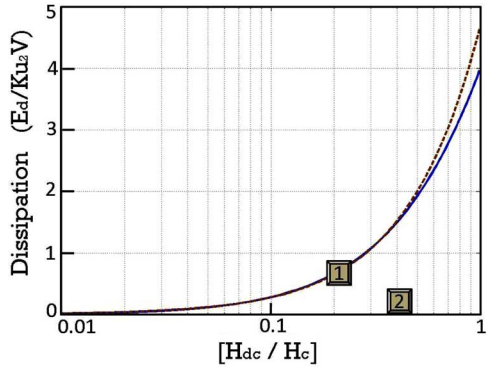

Fig. 6. Total dissipation under adiabatic switching with nonzero bias. There is no dissipation associated with *case 2* and dissipation of *case 1* for small (relevant) values of $H_{\rm dc}/H_c$ is less than the barrier height Ku_2V. The dashed line is plotted using (7).

for this saturating value of dissipation. Instead, we have numerically plotted dissipation versus $H_{\rm dc}/H_c$ (solid curve in Fig. 6). For small values of $H_{\rm dc}/H_c$, dissipation can be written as

$$E_d = \left(\frac{2H_{\rm dc}}{H_c}\right)^p (2Ku_2V) \ \ (p \approx 1.23) \tag{7}$$

where the value of p is obtained by an almost perfect fit to the solid curve for $H_{\rm dc} \leq 0.1H_c$. The dashed curve is plotted using (7). As is evident from Fig. 6, this equation is fairly accurate. There is some digression from the actual value of dissipation for large values of $H_{\rm dc}/H_c$ that are not of practical interest, especially $H_{\rm dc}/H_c = 1$ for which $H_{\rm dc}$ alone can switch the magnet and is completely an unwanted situation (see footnote 2).

It is important to note that the switching energy in the adiabatic limit is case-dependent. For *case 1*, it is given by (7) and is not zero as it might have been expected for dissipation in the adiabatic limit. Interestingly, if p was equal to 1, the dissipation would be equal to the energy difference between initial and final states [see points $1'$ and $4'$ in Fig. 5(b)]. However, the actual value is significantly smaller.

Dissipation in both the fast and slow limits can be casted into a single equation

$$E_d = \left(\frac{\tilde{H}}{H_c}\right)^p (2Ku_2V). \tag{8}$$

In the fast limit, $\tilde{H}$ is the magnitude of the pulse while in the slow limit, $\tilde{H}$ is related to the magnitude of the small bias field, as stated above. Ku_2V is the height of the anisotropy energy barrier separating the two stable states of the magnet, and has to be large enough so that the magnet retains its state while computation is performed without thermal fluctuations being able to flip it. The retention time for a given Ku_2V can be calculated using [21]–[23] $t_r = t_0\, e^{Ku_2V/kT}$, where t_0^{-1} is the attempt frequency with the range 10^9–$10^{12}\mathrm{s}^{-1}$ [22], [24] that depends in a nontrivial fashion on variables like anisotropy, magnetization, and damping.

IV. Magnetization Dynamics: Single Magnet

Thus far, we have shown switching energy in the two limiting cases of $\tau_r \ll \tau_c$ and $\tau_r \gg \tau_c$. To understand how switching energy changes in between and also how fast it decreases, we need to start from the LLG equation, which in the Gilbert form reads

$$\frac{d\vec{M}}{dt} = -|\gamma|\vec{M} \times \vec{H} + \frac{\alpha}{|\vec{M}|}\vec{M} \times \frac{d\vec{M}}{dt} \tag{9}$$

And in the standard form reads

$$(1+\alpha^2)\frac{d\vec{M}}{dt} = -|\gamma|(\vec{M} \times \vec{H}) - \frac{\alpha|\gamma|}{|\vec{M}|}\vec{M} \times (\vec{M} \times \vec{H}) \tag{10}$$

γ is the gyromagnetic ratio of electron and its magnitude is equal to $2.21 \times 10^5\,(\mathrm{rad}\cdot\mathrm{m})\cdot(\mathrm{A}\cdot\mathrm{s})^{-1}$ in SI and $1.76 \times 10^7\,\mathrm{rad}\cdot(\mathrm{Oe}\cdot\mathrm{s})^{-1}$ in CGS system of units, α is the phenomenological dimensionless Gilbert damping constant, and $\vec{M}$ is the magnetization. Here, $\vec{H} = \vec{H}_{\rm ani} + \vec{H}_{\rm pulse}$, where $\vec{H}_{\rm ani} = (2Ku_2/M_s)m_z\hat{z}$. In general, $\vec{H}$ can be derived as the overall effective field: $\vec{H} = -(1/M_sV)\vec{\nabla}_m E$.

The following expressions are all equivalent statements of dissipated power[4] [27]:

$$P_d = \vec{H}\cdot\frac{d\vec{M}}{dt} = \frac{\alpha}{|\gamma||\vec{M}|}\left|\frac{d\vec{M}}{dt}\right|^2 = \frac{\alpha|\gamma|}{(1+\alpha^2)|\vec{M}|}|\vec{M}\times\vec{H}|^2. \tag{11}$$

The dissipated power has to be integrated over time to give the total dissipation. In general, LLG can be solved numerically using the Runge–Kutta method. To obtain generic results that are the same for various parameters, we recast LLG and the dissipation rate into a dimensionless form. This will also show the significance of τ_c and demonstrate why for ramp times exceeding $\tau_c = 1$, there is a significant drop in dissipation.

Using scaled variables $\vec{m} = \vec{M}/M_sV$ and $\vec{h} = \vec{H}/H_c$, (10) in dimensionless form can be written as

$$\frac{d\vec{m}}{dt'} = -\frac{1}{2\alpha}(\vec{m}\times\vec{h}) - \frac{1}{2}\vec{m}\times(\vec{m}\times\vec{h}) \tag{12}$$

where $t' = t/\tau_c$ with τ_c given by (14). The energy dissipation normalized to Ku_2V can be written as

$$\frac{E_d}{Ku_2V} = \frac{1}{Ku_2V}\int \vec{H}\cdot\frac{d\vec{M}}{dt}dt = \int 2\vec{h}\cdot\frac{d\vec{m}}{dt'}dt'. \tag{13}$$

To estimate the time constant involved in switching a magnet, it is instructive to plot (see Fig. 7) the integrand $2\vec{h}\cdot(d\vec{m}/dt') = (\tau_c/Ku_2V)\left(\vec{H}\cdot(d\vec{M}/dt)\right)$ appearing earlier in (13) assuming a step function for $H_{\rm pulse}$ and obtaining the corresponding $d\vec{m}/dt'$ from (12). Note that the integrands (Fig. 7) die out exponentially for a wide range of α's from 0.005 to 0.5. In other words, all the curves (ignoring the oscillations) can be approximately described by $e^{-t'} = e^{-t/\tau_c}$, thus suggesting that

[4]Note that the the term $\vec{M}\cdot(d\vec{H}_{\rm applied})/dt$ should not have been included in equation 4 of reference 1. However, this will not change the results of that paper since this term was assumed to be zero anyways.

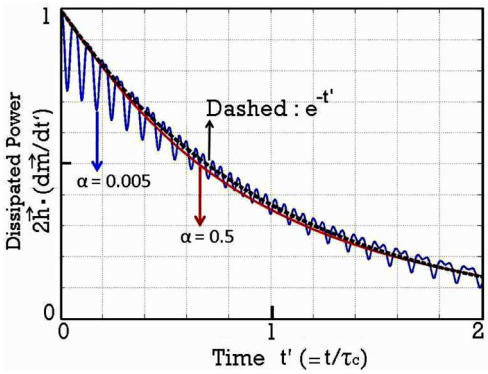

Fig. 7. Solid lines show the dissipated power $2\vec{h}\cdot(d\vec{m}/dt')$ under an instantaneous turn-ON of $H_{\rm pulse}$ to H_c for $\alpha = 0.005$ and $\alpha = 0.5$. Dashed line shows an exponential decay $e^{-t'}$. This figure shows that although the value of α changes the time (with real dimensions) at which the dissipated power decreases to $1/e$ through changing τ_c, it does not affect the functional form of the decay that is more or less an exponential decay even if α changes by 2 orders of magnitude.

the approximate time constant is τ_c

$$\tau_c = \frac{1+\alpha^2}{2\alpha(|\gamma|H_c)}. \tag{14}$$

This is more evident from Fig. 8, where we show the energy dissipation for pulses with different ramp times. The dissipated energy drops when τ_r exceeds τ_c as we might expect, but the drop is sharper than an *RC* circuit. Needless to say, the dissipation values calculated from LLG equation for the two limits of fast pulse ($\tau_r \ll \tau_c$) and adiabatic pulse ($\tau_r \gg \tau_c$) are consistent with the values calculated using energetics previously. Fig. 8(a) shows the *turn*-ON dissipation where *case 1* has saturated and *case 2* goes down as ramp time is increased. The curve in the middle is the case with infinitesimal bias $H_{\rm dc} = 0$ and it is just provided for reference. Fig. 8(b) shows the *turn*-OFF dissipation where both cases 1 and 2 dissipate arbitrarily small amounts as the ramp time is increased. With slow pulses, overall switching energy of *case 2* is very small and the entire switching energy of *case 1* essentially occurs during *turn*-ON that is illustrated in Fig. 8(c). This dissipation was discussed in Section III-B, and it is associated with the sudden fall down from point A to B [see Fig. 5(b) and (c)]. It has a saturating nature and will never become zero. As $H_{\rm pulse}$ is applied more and more gradually, the dissipated power in Fig. 8(c) becomes narrower and taller. In the true adiabatic limit, it will become a delta function occurring for one particular value of $H_{\rm pulse}$.

V. Magnetization Dynamics: Chain of Inverters

Fig. 9(a) shows an array of spherical nanomagnets (MQCA) that interact with each other via dipole–dipole coupling [32]. The objective is to determine the switching energy if we are to switch magnet 2 according to the state of magnet 1 (see footnote 2). In Section V-A, we will show a clocking scheme under which propagation of information can be achieved and basically shows how magnets can be used as *cascadable logic* building blocks. In Section V-B, we briefly go over the method and equations used to simulate the dynamics and dissipation of the coupled magnets. In Section V-C, we analyze the dissipation of the chain of inverters where we show that after cascading the magnetic bits, dissipation changes linearly with the number of magnets that the pulse is exerted on. This shows that the intrinsic switching energy of larger more complicated circuits can be calculated using the one-magnet results presented in this paper, at least approximately.

A. Clocking Scheme

In Section I, we mentioned that in the clocking scheme the role of the clock field is to provide energy whereas field of another magnet acts as a guiding input. Using a clock we can operate an array of exactly similar magnets as a chain of inverters. Fig. 9(a) shows a three-phase inverter chain where the unit cell is composed of three magnets. Each magnet has two stable states showed as *up* and *down* in the figure. We want to switch magnet 2 according to the state of magnet 1. First, consider only magnets 1 and 2. We have already explained (see Section I) how magnet 1 can determine the final state of magnet 2. But what happens if more magnets are present?

Consider magnets 1–3. Just like magnet 1, magnet 3 also exerts a field on magnet 2 and if it is in the opposite direction can cancel out the field of magnet 1. To overcome this, we apply the pulse to magnet 3 as well, thereby diminishing the exerted z field of magnet 3 on magnet 2 so that magnet 1 becomes the sole decider of the final state of magnet 2. In the process, the data in magnet 3 has been destroyed (it will end up wherever magnet 4 decides). It takes three pulses to transfer the bit (in an inverted manner) in magnet 1 to magnet 4. Magnet 4 has been included because it affects the dissipation of magnet 3 through affecting its dynamics. Inclusion of more magnets to the right or left of the array will not change the quantitative or qualitative results of this paper. Next, we will briefly go over the method used to simulate the chain of inverters.

B. Numerical Simulation of the Chain of Inverters

Equations (12) and 13 are used to simulate the dynamics and dissipation of each magnet, respectively. The overall scaled (divided by H_c) magnetic field $\vec{h}$ of (12) for each magnet at each instant of time is modified to

$$\vec{h} = \frac{\vec{H}_{\rm pulse} + \vec{H}_{\rm ani} + \vec{H}_{\rm dip}}{H_c} \tag{15}$$

composed of the applied pulse

$$\vec{H}_{\rm pulse} = H_{\rm pulse}\hat{y} \tag{16}$$

the anisotropy (internal) field of each magnet

$$\vec{H}_{\rm ani} = \frac{2Ku_2}{M_s} m_z \hat{z} \tag{17}$$

and exerted dipolar fields of other magnets that, in general, in CGS system of units reads

$$\vec{H}^j_{dip} = \sum_{n\neq j} \frac{3\,(\vec{\mu}_n \cdot \vec{r}_{nj})\,\vec{r}_{nj} - \vec{\mu}_n r^2_{nj}}{r^5_{nj}}. \tag{18}$$

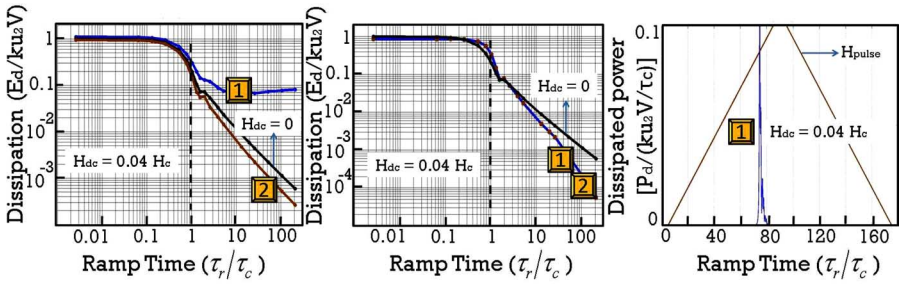

Fig. 8. (a) *Turn*-ON dissipation versus ramp time. As ramp time is increased, dissipation in *case 2* decreases arbitrary but it saturates in *case 1*. In both cases, there is a significant drop in dissipation once the ramp time exceeds τ_c. (b) *Turn*-OFF dissipation versus ramp time. In both cases, dissipation can be made arbitrarily small by increasing the ramp time. Again, there is a significant drop in dissipation as ramp time exceeds τ_c. (c) Dissipated power versus ramp time. This figure shows that in the slow limit of switching, for *case 1* that has a saturating switching energy, the dissipated power essentially occurs during *turn*-ON. This fact was discussed earlier in Fig. 5(b) and (c) as the dissipation between points A and B during turn-ON. If adiabatic limit of switching is really reached, then the dissipated power in this figure will become a very sharp spike.

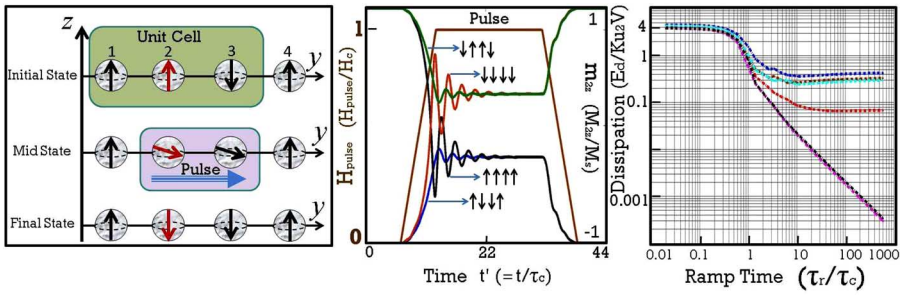

Fig. 9. (a) Array of identical nanomagnets with uniaxial anisotropy and easy axis along z coupled together via dipolar coupling that can be operated as a three-phase inverter chain. Initially, the four-magnet array can be randomly in any of the 16 possible states. A unit cell is composed of three magnets with the real information stored in magnet 1 in the initial state. A y pulse provides energy and puts magnets 2 and 3 in the mid state, thereby shutting OFF the z field of magnet 3 on 2, so that field of magnet 1 can deterministically tilt magnet 2 downward. Upon removing the pulse, magnet 2 relaxes down in the final state. (b) LLG simulation of coupled system of (a). This figure shows the proper operation of the clocking scheme by showing the normalized magnetization of magnet 2 along its easy axis for various initial configurations. (c) Dissipation of the array as a function of ramp time. There are $\binom{4}{2} = 6$ physically distinct configurations out of 16 possible states. The dissipation is lower if the initial configuration minimizes the energy of dipolar interaction. Assigning binary 1 to $\uparrow$ and binary 0 to $\downarrow$ the 6 curves (from highest to lowest) represent these configurations: 1) 0, 15; 2) 1, 7, 8, 14; 3) 3, 12; 4) 2, 4, 11, 13; 5) 6, 9; and 6) 5, 10.

All field values are time-dependent. Here, j denotes any one magnet and μ_n runs over magnetic moments of the other magnets. Though this equation can be simplified for an array of magnets along the same line, in this form it can be used for more complicated arrangement of magnets. Fig. 9(b) shows the LLG simulations of the chain of inverters where magnet 2 is switched solely according to the state of magnet 1 irrespective of its history or the state of magnets 3 and 4.

C. Dissipation of the Chain of Inverters With one Application of the Pulse

Fig. 9(c) shows dissipation of the entire array after one application of the pulse as a function of ramp time. The pulse is exerted on magnets 2 and 3 that accounts for the $4Ku_2V$ value in the fast limit. This essentially points out that after cascading these logic building blocks, dissipation changes linearly with the number of magnets.

In the slow limit, depending on the initial configuration, dissipation will be affected. The four-magnet array can initially be in any of its 16 possible states. Some configurations saturate and some do not. Here, the field of magnet 1 plays the role of the bias field $H_{\rm dc}$ for magnet 2 and the field of magnet 4 is like another bias field on magnet 3 that accounts for the three groups of curves in Fig. 9(c). The upper curves correspond to the situation where initial magnetization of both magnets 2 and 3 are opposite to the fields exerted from magnets 1 and 4, respectively. The middle curves correspond to only one of magnets 2 or 3 initially being opposite to the exerted fields of magnet 1 or 4, respectively. The lower curves correspond to both magnets 1 and 3, initially being in the same direction as the exerted fields from magnets 2 and 4, respectively.

An added complication is the field of the other neighbor (magnet 3) that is diminished in the z-direction but has a nonnegligible y component exerted on magnet 2. All of this y-directed field does is to wash away a tiny bit the effect of the field of magnet 1 that has little bearing on the qualitative or quantitative results, as illustrated in Fig. 9(c).

VI. Discussion and Practical Considerations

A. Dissipation Versus Speed

The speed of switching can be increased by increasing the magnitude of the external pulse $H_{\rm pulse}$ above H_c. Larger fields

will dissipate more energy but have the advantage of aligning the magnet faster during the turn-ON segment but are of no use for increasing the speed of the turn-OFF segment because the magnet relaxes to its stable state under its own internal field. If $H_c = 2Ku_2V/M_sV$ can be altered, then it is a better idea to increase H_c and always set $H_{\rm pulse} = H_c$. This way the speed of switching is increased by shortening the time of both turn-ON and turn-OFF segments.

B. Increasing the Switching Speed

From (14), it can be concluded that increasing α shortens the switching time constant (note that α is usually less than 1); however, this parameter is not very controllable in experiments. $|\gamma|$ is a physical constant (at least in ordinary materials) and cannot be altered. So, to increase the switching speed, one has to increase $H_c = 2Ku_2V/M_sV$. Thermal stability of a magnet requires Ku_2V to be larger than a certain amount for the desired retention time. For instance, with an attempt frequency of about 1 GHz (see the discussion at the end of Section III) and Ku_2V of about 0.5 eV, magnet is stable for about 0.5 s that is large enough because switching takes place in the nanosecond scale. A higher retention time requires higher Ku_2V. Once Ku_2V is set because of stability requirements, the only way to increase H_c is to decrease M_sV. Assuming that volume is magnetized to saturation, $M_sV = N_s\mu_B$ is the magnetic moment of the magnet. N_s is the number of spins giving rise to the magnetization and μ_B is Bohr magneton. So, decreasing M_sV translates to making the magnet smaller or decreasing its saturation magnetization.

The discussion just presented is similar to the theory of scaling in CMOS technology where decreasing the capacitance causes an increase in the switching speed by decreasing the RC time constant. With the same operating voltage, smaller capacitance results in lower number of charges stored on the capacitor. In the case of CMOS, as C decreases, energy dissipated, i.e., $0.5CV^2$ also decreases. In the case of magnet, however, energy dissipation is fixed around $2Ku_2V$; so, for a lower M_sV, dissipation of the ferromagnetic logic element (already very small) is *not* altered; however, one might be able to reduce the dissipated energy in the external circuitry since it needs to provide the energy for a shorter period of time. Again, we should emphasize that a thorough analysis of external dissipation also has to be done. This has to do with generating the external source of energy for switching. In the case of MQCA circuits, this is done by running currents through wires and generating magnetic fields. In principle, spin-transfer torque phenomena or electrically controlled multiferroicity could also be used to provide the source of energy. These methods would also have energy dissipation associated with them.

C. Integration Density

A complete circuit layout is necessary to properly evaluate the integration density of logic circuits made of magnets. For example, fringing fields and unwanted crosstalks have to be taken into account. External circuitry will take up space and dissipate energy. Efficient methods have to be developed to properly address these issues. One component of the layout is the magnetic logic bit itself that we discuss here. The barrier height $E_b = Ku_2V$ between the stable states of a magnet can be engineered by adjusting Ku_2 (anisotropy constant) and V (volume). Increasing the anisotropy constant is of great interest for the magnetic storage industry because it allows stable magnets of smaller volume that translates into higher densities. Many experiments report Ku_2 values on the order of a few $10^7 \mathrm{erg/cm^3}$ (see, e.g., [28]–[30]). This results in stable magnets with volumes of only tens of cubic nanometers, which means that stable magnets can be made as small as a few nanometers in each dimension. Even though a complete layout is necessary, nevertheless, these numbers are very promising and could potentially result in very high integration densities.

VII. Conclusion

In this paper, we analyzed the switching energy of single-domain nanomagnets used as cascadable logic building blocks. A magnetic pulse was used to provide the energy for switching and a bias field was used as an input to guide the switching. The following conclusions can be drawn from this study.

1) Through analyzing the complete dependence of the switching energy on ramp time of the pulse, it was concluded that there is a significant and sharp drop in dissipation for ramp times that exceed a critical time given by (14) whose significance is separating the energy dissipation characteristic of a fast pulse (small ramp time) and energy dissipation characteristic of a slow pulse (large ramp time).
2) The switching energy can be described by a single equation [(8)] in both fast and slow limits for trapezoidal pulses analyzed in this paper. In the fast limit, the effect of the bias field, or equivalently, the field of neighboring magnet in MQCA systems is negligible so long as the bias field is less than tenth of the switching field of the magnet. In the slow limit, however, dissipation is largely determined by the value of the bias field.
3) By evaluating switching energy of both one magnet and a chain of inverters for MQCA systems, it was shown that the switching energy increases linearly with the number of magnets so that the one magnet results provided in this paper can be used to calculate the switching energy of larger more complicated circuits, at least approximately.
4) Practical issues such as dissipation versus speed, increasing the switching speed, and scaling were discussed qualitatively. It was concluded that by proper designing, ferromagnetic logic bits can have scaling laws similar to the CMOS technology.

Noise was not directly included in the models; however, we took it into account indirectly: thermal noise is the limiting factor on the anisotropy energy barrier Ku_2V of a magnet that we discussed thoroughly. Thermal noise also limits the lowest possible magnitude of the bias field (or equivalently coupling between magnets in MQCA systems). We have provided the results for a wide range of bias values. More thorough discussions

of dissipation in the external circuitry can be found in references [13], [14], and [33].

ACKNOWLEDGMENT

Authors would like to thank Dr. D. Nikonov of Intel Corporation and Prof. S. Bandyopadhyay for fruitful discussions.

REFERENCES

[1] S. Salahuddin and S. Datta, "Interacting systems for self correcting low power systems," *Appl. Phys. Lett.*, vol. 90, pp. 093503-1–093503-3, Feb. 2007.

[2] R. P. Cowburn and M. E. Welland, "Room temperature magnetic quantum cellular automata," *Science*, vol. 287, pp. 1466–1468, Feb. 2000.

[3] R. P. Cowburn, A. O. Adeyeye, and M. E. Welland, "Controlling magnetic ordering in coupled nanomagnet arrays," *New J. Phys.*, vol. 1, pp. 16-1–16-9, Nov. 1999.

[4] A. Imre, G. Csaba, L. Ji, A. Orlove, G. H. Bernstein, and W. Porod, "Majority logic gate for magnetic quantum-dot cellular automata," *Science*, vol. 311, pp. 205–208, Jan. 2006.

[5] A. Ney, C. Pampuch, R. Koch, and K. H. Ploog, "Programmable computing with a single magnetoresistive element," *Nature*, vol. 425, pp. 485–487, Oct. 2003.

[6] D. A. Allwood, G. Xiong, M. D. Cooke, C. C. Faulkner, D. Atkinson, N. Vernier, and R. P. Cowburn, "Submicrometer ferromagnetic NOT gate and shift register," *Science*, vol. 296, pp. 2003–2004, Jun. 2002.

[7] D. A. Allwood, G. Xiong, C. C. Faulkner, D. Atkinson, D. Petit, and R. P. Cowburn, "Magnetic domain-wall logic," *Science*, vol. 309, pp. 1688–1692, Sep. 2002.

[8] D. E. Nikonov, G. I. Bourianoff, and P. A. Gargini. (2007, Nov.). Simulation of highly idealized, atomic scale MQCA logic circuits [Online]. Available: http://arxiv.org/, arXiv:0711.2246v1 [cond-mat.mes-hall].

[9] G. Csaba, W. Porod, and A. I. Csurgay, "A computing architecture composed of field-coupled single domain nanomagnets clocked by magnetic field," *Int. J. Circ. Theor. Appl.*, vol. 31, pp. 67–82, Jan. 2003.

[10] G. Csaba, A. Imre, G. H. Bernstein, W. Porad, and V. Metlushko, "Nanocomputing by field-coupled nanomagnets," *IEEE Trans. Nanotech.*, vol. 1, no. 4, pp. 209–213, Dec. 2002.

[11] G. Csaba, P. Lugli, and W. Porod, "Power dissipation in nanomagnetic logic devices," in *Proc. 4th IEEE Conf. Nanotechnol.*, Aug. 2004, pp. 346–348.

[12] G. Csaba, P. Lugli, A. Csurgay, and W. Porod, "Simulation of power gain and dissipation in field-coupled nanomagnets," *J. Comp. Elec.*, vol. 4, pp. 105–110, Aug. 2005.

[13] M. Niemier, M. Alam, X. S. Hu, G. Bernstein, W. Porod, M. Putney, and J. DeAngelis, "Clocking structures and power analysis for nanomagnet-based logic devices," in *Proc. 2007 Int. Symp. Low Power Electron. Design (ISLPED)*. New York: ACM, pp. 26–31.

[14] D. E. Nikonov, G. I. Bourianoff, and P. A. Gargini, "Power dissipation in spintronic devices out of thermodynamic equilibrium," *J. Super. Novel. Magn.*, vol. 19, no. 6, pp. 497–513, Aug. 2006.

[15] L. Landau and E. Lifshitz, "On the theory of the dispersion of magnetic permeability in ferromagnetic bodies," *Phys. Z. Sowjetunion*, vol. 8, pp. 153–169, 1935.

[16] T. L. Gilbert, "A phenomenological theory of damping in ferromagnetic materials," *IEEE Trans. Magn.*, vol. 40, no. 6, pp. 3443–3449, Nov. 2004.

[17] B. Hillebrands and K. Ounadjela, Eds., *Spin Dynamics in Confined Magnetic Structures I, II and III*. New York: Springer-Verlag, 2001–2007.

[18] C. H. Bennet, "The thermodynamics of computation — a review," *Intern. J. Theor. Phys.*, vol. 21, pp. 905–940, Dec. 1982.

[19] K. K. Likharev and A. N. Korotkov, "Single-electron parametron: Reversible computation in a discrete-state system," *Science*, vol. 273, pp. 763–765, Aug. 1996.

[20] R. K. Kummamuru, A. O. Orlov, R. Ramasubramaniam, C. S. Lent, G. H. Bernstein, and G. Snider, "Operation of a quantum-dot cellular automata (QCA) shift register and analysis of errors," *IEEE Trans. Electron Devices*, vol. 50, no. 9, pp. 1906–1913, Sep. 2003.

[21] R. Street and J. C. Woolley, "A study of magnetic viscosity," *Proc. Phys. Soc., Sec. A*, vol. 62, pp. 562–572, Sep. 1949.

[22] L. Neel, "Thermoremanent magnetization of fine powders," *Rev. Mod. Phys.*, vol. 25, pp. 293–295, Jan. 1953.

[23] W. F. Brown, "Thermal fluctuations of a single-domain particle," *Phys. Rev.*, vol. 130, pp. 1677–1686, Jun. 1963.

[24] P. Gaunt, "The frequency constant for thermal activation of a ferromagnetic domain wall," *J. Appl. Phys.*, vol. 48, pp. 3470–3474, Aug. 1977.

[25] H. S. Leff and A. F. Rex, *Maxwell's Demon 2*. Bristol, Philadelphia: Inst. Phys. (IoP), 2003.

[26] R. K. Cavin III, V. V. Zhirnov, J. A. Hutchby, and G. I. Bourianoff, "Energy barriers, demons, and minimum energy operation of electronic devices (plenary paper)," *Proc. SPIE*, vol. 5844, pp. 1–9, May 2005.

[27] Z. Z. Sun and X. R. Wang, "Fast magnetization switching of Stoner particles: A nonlinear dynamics picture," *Phys. Rev. B*, vol. 71, pp. 174430-1–174430-9, May 2005.

[28] S. Sun, C. B. Murray, D. Weller, L. Folks, and A. Moser, "Monodisperse FePt nanoparticles and ferromagnetic FePt nanocrystal superlattices," *Science*, vol. 287, pp. 1989–1992, Mar. 2000.

[29] X. W. Wu, C. Liu, L. Li, P. Jones, R. W. Chantrell, and D. Weller, "Nonmagnetic shell in surfactant-coated FePt nanoparticles," *J. Appl. Phys.*, vol. 95, no. 11, pp. 6810–6812, Jun. 2004.

[30] A. Perumal, H. S. Ko, and S. C. Shin, "Magnetic properties of carbon-doped FePt nanogranular films," *Appl. Phys. Lett.*, vol. 83, no. 16, pp. 3326–3328, Oct. 2003.

[31] K. Elkins, D. Li, N. Poudyal, V. Nandwana, Z. Jin, K. Chen, and J. P. Liu, "Monodisperse face-centered tetragonal FePt nanoparticles with giant coercivity," *J. Phys. D: Appl. Phys.*, vol. 38, pp. 2306–2309, Jul. 2005.

[32] J. D. Jackson, *Classical Electrodynamics*. New York: Wiley, 1999, pp. 198–200.

[33] C. Augustine, X. Fong, B. Behin-Aein, and K. Roy, "A design methodology and device/circuit/architecture compatible simulation framework for low-power magnetic quantum cellular automata systems," in *Proc. ASPDAC*, 2009, pp. 847–852.

Authors' photographs and biographies not available at the time of publication.